

Article

Exploiting Growing Stock Volume Maps for Large Scale Forest Resource Assessment: Cross-Comparisons of ASAR- and PALSAR-Based GSV Estimates with Forest Inventory in Central Siberia

Christian Hüttich ^{1,*}, Mikhail Korets ², Sergey Bartalev ³, Vasily Zharko ³, Dmitry Schepaschenko ⁴, Anatoly Shvidenko ⁴ and Christiane Schmullius ¹

¹ Department for Earth Observation, Friedrich-Schiller-University Jena, Löbdergraben 32, 07743 Jena, Germany; E-Mail: c.schmullius@uni-jena.de

² Sukachev Institute of Forest, Siberian Branch of the Russian Academy of Sciences, Krasnoyarsk, 660036, Russia; E-Mail: mik@ksc.krasn.ru

³ Space Research Institute of the Russian Academy of Sciences, Moscow 117997, Russia; E-Mails: bartalev@d902.iki.rssi.ru (S.B.); zharko@d902.iki.rssi.ru (V.Z.)

⁴ International Institute for Advanced System Analyses, Laxenburg 2361, Austria; E-Mails: schepd@iiasa.ac.at (D.S.); shvidenk@iiasa.ac.at (A.S.)

* Author to whom correspondence should be addressed; E-Mail: Christian.huettich@uni-jena.de; Tel.: +49-3641-948886; Fax: +49-3641-948882.

Received: 12 March 2014; in revised form: 24 June 2014 / Accepted: 7 July 2014 /

Published: 22 July 2014

Abstract: Growing stock volume is an important biophysical parameter describing the state and dynamics of the Boreal zone. Validation of growing stock volume (GSV) maps based on satellite remote sensing is challenging due to the lack of consistent ground reference data. The monitoring and assessment of the remote Russian forest resources of Siberia can only be done by integrating remote sensing techniques and interdisciplinary collaboration. In this paper, we assess the information content of GSV estimates in Central Siberian forests obtained at 25 m from ALOS-PALSAR and 1 km from ENVISAT-ASAR backscatter data. The estimates have been cross-compared with respect to forest inventory data showing 34% relative RMSE for the ASAR-based GSV retrievals and 39.4% for the PALSAR-based estimates of GSV. Fragmentation analyses using a MODIS-based land cover dataset revealed an increase of retrieval error with increasing fragmentation of the landscape. Cross-comparisons of multiple SAR-based GSV estimates helped to detect

inconsistencies in the forest inventory data and can support an update of outdated forest inventory stands.

Keywords: forest inventory; biomass; ALOS PALSAR; ENVISAT ASAR; land cover fragmentation; Siberia; boreal forest management

1. Introduction

Forests play a pivotal role in Earth's carbon balance. Hence our ability to fully understand and quantify the impact that vast forests have on the global environment is important for the monitoring of international agreements aimed at CO₂ reductions. The forests in Central Siberia are important carbon sinks [1–4]. Quantifying the state and dynamics of above ground biomass is of utmost importance for forest resource management on local and regional scale administrative levels. However, more than 25% of the Russian forest inventory has not been updated in the last 25 years. Moreover, human and environmental forest disturbances continuously change forest cover and biomass distribution. The magnitude and extent of on-going environmental pressures (e.g., forest fragmentation and the impact of global climate change) and the loss rates of particular habitat types is not known in detail in Central Siberia. Forest management administrations, forest-related industry [4,5], and the carbon modeling community rely on updated and correct data on forest distribution and carbon stocks [6,7]. However, the existing forest inventory data is often outdated, not consistent in terms of accuracy and reliability on national level, and of restricted access.

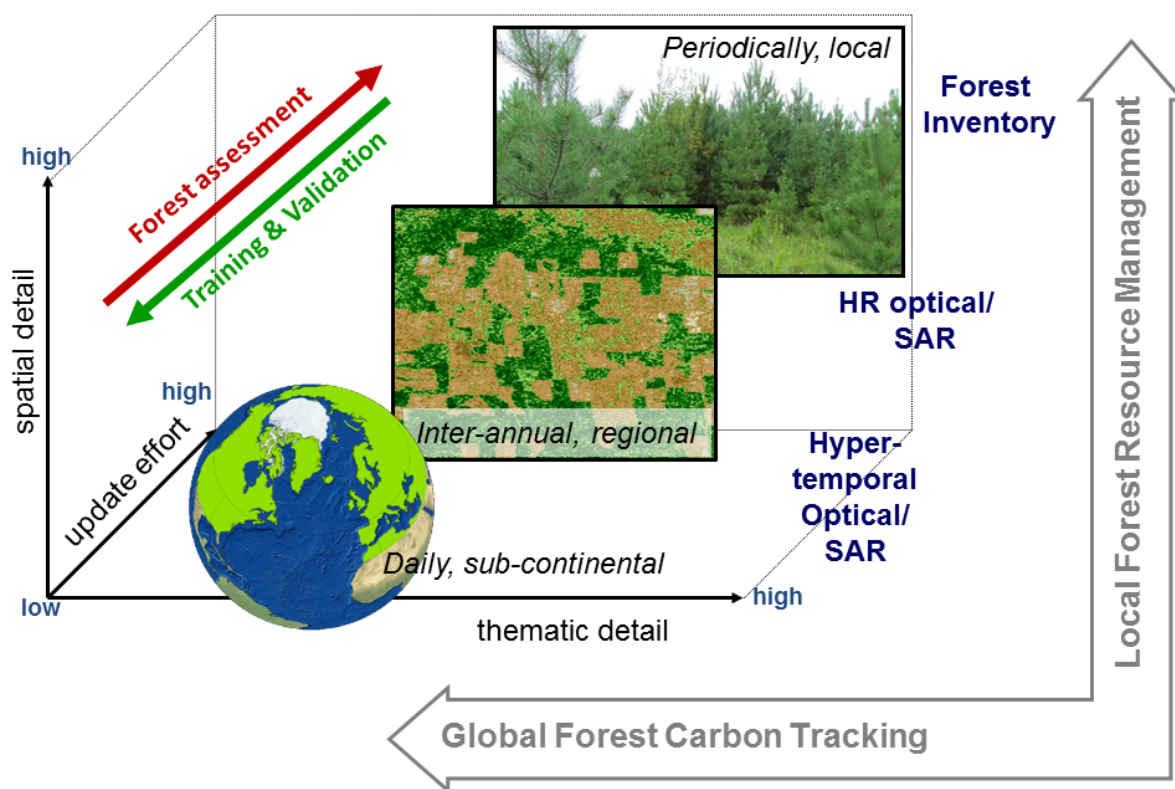
Biomass is one of the considered Essential Biodiversity and Climate Variables (ECV, EBV [8]). Growing stock volume (GSV) is densely correlated with above ground biomass of forest ecosystems. In addition, the availability of a system of regression equations between all live biomass components (stems, branches, foliage, roots, understory, and green forest floor) allows to assess the entire biomass of forest ecosystems based on remotely sensed GSV [1]. Thus, GSV is the key parameter for full terrestrial carbon accounting. A deeper understanding of satellite-based above-ground biomass assessment at different scales would allow for a significant reduction of uncertainties in forest carbon cycling assessment. Important research needs have to be addressed for a better representation of GSV estimates in carbon accounting models by implementing timely earth observation data and improving the spatial resolution of the model input parameters, as stated by [3].

Forest biomass assessment and monitoring requires a sound uncertainty analysis, in particular for comparing geo-information of forest stock maps at different spatial scales. However, a proper accuracy assessment between satellite-based maps and forest inventory is often problematic due to high expenses for ground truth measurements, limited access to existing statistical data and restrictions for delivery of *in situ* data. Capabilities and limitations of up- and downscaling above-ground biomass geo-information products are still not completely understood and require strong interdisciplinary interactions. For several decades, remotely sensed data have aided many aspects of forest monitoring [9]. Besides optical space borne systems, such as LIDAR [10], Landsat [11,12], and IRS [13] up-to-date earth observation data sources and techniques have improved in the last decade. For instance, multi-temporal SAR-based data can provide biophysical information on forest growing stock retrieval

algorithms [14,15]. The application of SAR systems in combination with the multidimensional system of forest biomass structure is a crucial tool for updating obsolete forest inventories and forest regrowth after disturbances [15–17]. The development of spatiotemporally more detailed and accurate biomass maps including land use and land cover change information is a pre-condition for more accurate carbon accounting and net primary production assessments. There is also a need for inter-comparison and (cross-) validation assessments of independently derived GSV estimates since SAR data are being delivered spatially consistent at continental [18], pan-boreal [19] or global scale [20].

Further research has to be initiated in the field of satellite-based multi-source forest resource assessment (as indicated in various studies [21–23]). Specifically, integrated concepts for forest characterization based on remote sensing (Figure 1) have to be developed to assess the agreement, accuracy, and transferability of forest resource maps for large area forest management purposes.

Figure 1. Integrated concept for forest resource assessment and forest geo-information cross validation; the graph exemplarily indicates the range of data specifications in terms of spatial and thematic detail in relation to the effort of frequent update.



A principle goal is to overcome existing gaps of inadequate data integration and interoperability as stated as one of the targeted gaps by GEO [24]. In the context of operational forest ecosystem monitoring and forest resource assessment, important research questions arising are: How comparable are SAR derived GSV datasets at different scales, derived with different SAR systems and modeling approaches; and to what extent can SAR-based GSV retrievals and forest inventory data from different regions be compared to one another?

The aim of this paper is to:

- cross-compare GSV maps derived from ALOS-PALSAR (25 m, L-band) data and ENVISAT ASAR (1 km, C-band) backscatter data with updated forest inventory maps for test sites in Central Siberia, and
- analyze the effects of forest cover type and landscape fragmentation on the spatial congruence of multi-scale GSV maps.

2. Study Area and Data

2.1. Forest Inventory Data of Central Siberia Test Sits

In situ data were available from three forest management areas in Central Siberia (referred to as test sites) covering an area of 2,049,629 ha (Table 1). The location and spatial distribution is shown in Figure 2. The dataset consists of a digital map of forest stands and several strata of forest variables (land cover type, species composition, tree density, average age, height, diameter, and GSV). A forest stand is defined as an elementary forest inventory unit (EFIU), a forest area relatively homogeneous in vegetation structure and growing conditions. According to the Russian forest inventory regulations [25], forest stands are delineated and described by a forest inventory expert on 1:10,000 scales by using multispectral airborne images and auxiliary reference field data. The average is 17 ha with a standard deviation of 21.5 ha. The minimum size of all forest stands within the study area was four ha.

Table 1. Test sites.

Site №	Site Name (Forest Management Area)	Area, ha	Number of EFIU	Region
1	Kazachinsk and Bolshemurtinsk	943,494	51,804	Krasnoyarsk Kray
2	Abansk and Dolgomostovsk	727,139	45,424	Krasnoyarsk Kray
3	Padunsk	378,996	23,408	Irkutsk Oblast
	Total	2,049,629	120,636	

Figure 2. Location of the test sites in Central Siberia.



2.2. ALOS PALSAR

Spatially explicit estimates of GSV with a pixel size of 25 m were obtained from Advanced Land Observing Satellite (ALOS) Phased Array type L-band SAR (PALSAR) images. ALOS PALSAR operated between 2006 and 2011 at L-band (wavelength of 23 cm) with a pre-defined acquisition plan aiming, among other, at a yearly wall-to-wall coverage of forests. The PALSAR dataset consisted of four yearly mosaics of the radar backscattered intensity acquired during summer and fall between 2007 and 2010 in the Fine Beam Dual (FBD) mode. In FBD mode, PALSAR acquired co-polarized (HH) and cross-polarized (HV) signals. For each year, the mosaic included images of the radar backscatter acquired during summer and fall because unfrozen conditions cause the backscatter to be most sensitive to forest structural parameters [26]. The PALSAR mosaics were obtained after SAR long strip processing, ortho-rectification, slope correction and neighboring strip suppression [27]. The mosaics were provided through JAXA's Kyoto and Carbon Science Initiative [28] in a ready-to-use format.

2.3. ENVISAT ASAR

Spatially explicit estimates of GSV with a pixel size of 1000 m were obtained from Envisat's Advanced Synthetic Aperture Radar (ASAR) images acquired in the ScanSAR mode between October 2009 and February 2011. ENVISAT ASAR operated between 2002 and 2012 at C-band (wavelength of 6 cm); ScanSAR mode, multiple images were acquired globally whenever resources were available. This led to a very dense archive of images. For the boreal zone almost daily observations were available.

2.4. MODIS

MODIS (MOD09GQ/GA) data were used to map land cover types at 230 m spatial resolution. The land cover map was obtained from time series of spectral reflectance composite images, corresponding to different seasons of the year and capturing the spatial-temporal variations in onset, peak and end of growing season as well as in the winter period (associated with snow cover [29,30]). Four MODIS-based seasonal image composites have been produced by temporal averaging of uncontaminated pixels for the spectral channels, such as spring (15 April 2010–15 June 2010), summer (15 June 2010–15 August 2010), autumn (15 August 2010–15 October 2010), and winter (15 November 2009–15 March 2010). For the winter image composite production snow cover related pixels have been involved into temporal averaging of surface reflectance values. Three seasonal composites, such as spring, summer and winter ones, have been produced for three (red, NIR and SWIR) spectral channels. The winter mosaic generation did not involve the SWIR channel due to its relatively high noise level.

3. Methods

3.1. Update and Quality Assessment of Forest Inventory Data

Since the forest stands were inventoried in the time period of 2001–2008, the database of *in situ* measurements was updated to account for vegetation cover changes up to 2011. Optical imagery from multiple sensors (LANDSAT TM, Resource-DK, Monitor-E, RAPIDEYE, QUICKBIRD, WORLDVIEW 1/2) were used. A GIS-based approach was used to check the consistency of the forest

inventory (FI) data with respect to the optical EO data. To minimize the impact of geolocation errors between the forest stand map and the EO data, a 30 m buffer was removed along the perimeter of each stand. A spatial homogeneity analysis based on mean and standard deviation (SD) of spectral band brightness values of 2010–2011 Landsat TM scenes was calculated for each EFIU. Forest stands with SD greater than two SD were assigned as change area and removed from the dataset of *in situ* measurements. The FI update identified 4% of the test sites as disturbed areas (logging and burned areas. To account for forest growth, stand age, height, diameter, relative density, and GSV, growth factors were applied on the *in situ* data based on reference growth tables of the tree species [31].

3.2. ALOS PALSAR Estimates of GSV

GSV was retrieved from the ALOS PALSAR mosaic data using a supervised random forest regression approach. Non-parametric tree-based ensemble regression techniques are widely used for ecological modeling [32–35]. The potential of random forest and bootstrap sampling to estimate forest variables was demonstrated in [9,17,36,37]. Random forest is a tree-based classifier where multiple trees are produced and combined based on equally weighted majority voting. A randomly selected third of the original training dataset is excluded for training each particular tree. This so-called out-of-bag (OOB) bootstrap sample is randomly permuted among the input features for each tree. With the remaining 2/3 of the training data, trees are grown to their maximal depth using the impurity *gini index* [38] due to the fact that the random permutation of samples and features antagonizes over fitting. In this study, the model was trained using GSV from the inventory database. A threshold of two standard deviations of GSV (m^3/ha) was applied on the training data to reduce effects of temporal mismatches like outdated FI data or eventually other occurring errors in SAR data (e.g., whether events leading to striping effects or saturation of the SAR backscatter signal in high volume forest stands [39–41]). As predictor variables, four annual HH and HV mosaics of backscattered intensity from 2007 to 2010 were used. An ensemble of 500 trees was grown per model run. The multi-temporal approach led to RMSE of $54.4 \text{ m}^3/\text{ha}$.

3.3. ENVISAT ASAR Estimates of GSV

A subset corresponding to the study area in Figure 2 has been extracted from the ENVISAT ASAR hyper-temporal backscatter series. The ASAR data preparations and the application of the hyper-temporal biomass retrieval algorithm contained the SAR processing of the ASAR GM imagery for the years 2009 and 2010 (geocoding, radiometric calibration, topographic normalization, speckle filtering, image tiling, MVA) and the application of the GSV retrieval algorithm. The following processing steps were performed by the BIOMASAR algorithm [14]: Training of water-cloud like backscatter model, model inversion and extraction of mono-temporal GSV maps, and multi-temporal combination of single GSV maps. As auxiliary data MODIS vegetation continuous field (VCF), a water mask, land cover, digital elevation model (SRTM) and maximum GSV from the literature were used. A detailed description of the BIOMASAR GSV retrieval is given in [14,15]. The ASAR backscatter time series were exploited to obtain spatially explicit estimates of GSV for latitudes above 30° N representative for the year 2010 with an accuracy of 40%–50% at pixel level and below 25% at aggregated level [15].

3.4. Land Cover Mapping

A locally-adaptive image classification method LAGMA (Locally-Adaptive Global Mapping Algorithm) [42] has been applied to recognize different land cover types using above mentioned seasonal image composites. The LAGMA method involves a regular grid based estimation of local (spectral and temporal) class signatures using spatially distributed reference data and supervised image classification. The LAGMA method inherently considers spatial variations of class features and allows the exploitation of the discriminative properties of local class signatures to the full extent without any preliminarily geographical stratification of mapping area. The obtained land cover map [43] consisted of 22 thematic classes, including 18 various vegetation types and 7 forest types defined based on their life forms, leaf types and phenology.

3.5. GSV Cross-Comparisons and Fragmentation Analyses

The ENVISAT-ASAR and ALOS-PALSAR estimates were cross-compared with respect to the updated FI data in order to analyze their characteristics terms of scales and land cover type. The PALSAR GSV map and the MODIS 250 m land cover map were resampled to the coarser 1 km resolution according to the ASAR GSV map. Cross-comparisons were stratified in terms of land cover and forest management area. Root Mean Square Errors (RMSE) were derived to quantify the congruency between the two datasets.

Table 2. Landscape fragmentation metrics used in this study using the Fragsats package [44].

Metric Name	Description
Mean Patch Size $MPS = (\sum_{i=1}^n a_{ij}^2) / n_i (1/10,000)$	Mean patch size indicates the mean size of all patches for a specific class in the landscape [44].
Shape index $SHAPE = (0.25 p_{ij}) / \sqrt{a_{ij}}$	“Shape index measures the complexity of patch shape compared to a standard shape. Mean shape index measures the average patch shape, or the average perimeter-to-area ratio, for a particular patch type (class) or for all patches in the landscape” [44]; p_{ij} = perimeter (m) of patch ij a = area (m) of patch ij .
Total (Class) Area $CA = \sum_{j=1}^n [a_{ij} (1/10,000)]$	“Total area equals the sum of the areas (m ²) of all patches of the corresponding patch type, a measure of landscape composition; specifically, how much of the landscape is comprised of a particular patch type” [44]; a = area (m) of patch ij .
Splitting Index $SPLIT = A^2 / (\sum_{i=1}^n a_{ij}^2)$	“Fragmentation indices based on the ability of two animals to get connected in a landscape; splitting index is defined as the number of patches in a landscape when dividing the total region into parts of equal size in such a way that this new configuration leads to the same degree of landscape division. Effective mesh size denotes the size of the areas when the region under investigation is divided into areas with the same degree of landscape division [45]; a = area (m) of patch ij . 2; A = total landscape area (m)
Effective Mesh Size $MESH = (\sum_{i=1}^n a_{ij}^2) / A (1/10,000)$	

The effects of landscape fragmentation on the RMSE were quantified by fragmentation indices according to [44]. Metrics as shown in Table 2 were derived based on the MODIS land cover dataset using the *ClassStat* function implemented in the R package Species Distribution Modeling Tools (*SDMTools*, [44]). Different fragmentation indices were generated indicating the fragmentation level of the forest land cover class distribution in the different test sites.

4. Results

4.1. Forest Inventory Update

The example in Figure 3 shows deforestation detected in a pair of SPOT-5 and WORLDVIEW-2 images between 2010 and 2011. The maximum and average GSV for each test site and for each major forest type are reported in Table 3. Siberian Pine and Scots Pine (in the following referred as Pine) exhibit the highest growing stock volume ranging from 360 m³/ha (Dolgomostowsk) to 480 m³/ha (Padunsk). Lowest maximum GSV on inventory unit level were estimated for Larch (290 m³/ha) in Kazachinsk and Fir (310 m³/ha) in Padunsk. Pine and Fir show increased variations in the average GSV between test sites. Disturbance activities were different between the test sites. Padunsk was characterized by old clear cuts (5400 ha, 2–10 years old with 2011 as reference year), Bolshemurtinsk and Kazachinsk were dominated by active cutting activities with 15,718 ha with an age of two years maximum.

Figure 3. Deforestation change detection based on SPOT-5 Pan (a: 26 July 2010) and WORLDVIEW-2 (b: RGB composite of a and c) satellite data. FI stands affected by forest cover change are indicated in b. The red polygons (c: 20 June 2011) indicate for cross-comparisons inadequate and disturbed FI stands as the result of the homogeneity analysis.

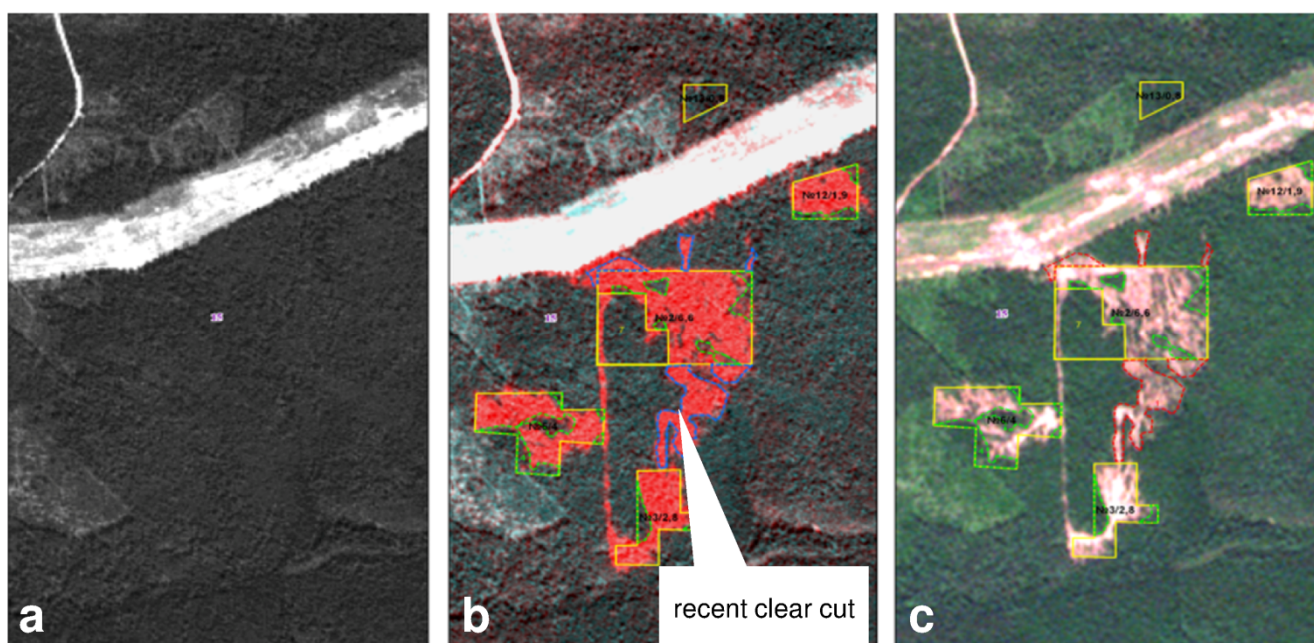


Table 3. Forest Inventory statistics for local test sites in Central Siberia.

Test Site	Padunsk		Bolshemurtinsk		Kazachinsk		Dolgomostovsk		Abansk	
	Avg m ³ /ha	Max m ³ /ha								
Land cover type										
Birch	109	280	122	320	118	270	103	320	96	270
Scots Pine	173	480	171	440	185	410	165	420	158	430
Aspen	132	330	169	450	149	380	157	380	178	340
Spruce	142	290	202	420	178	380	175	410	140	330
Fir	147	310	200	470	169	330	229	360	186	340
Larch	178	400	156	350	149	290	170	380	166	310
Siberian pine	102	400	269	520	240	400	191	360	275	450
Willow	39	90	39	90	17	35	49	60	26	40
Disturbances	Stands	Area (ha)								
Actual cutting (2010–2011)	0	0	10	197	23	316	6	57	5	29
Clear-cut (2002–2009)	475	5,416	649	15,718	160	2,618	181	1,408	526	3,692
Burned area (2002–2009)	67	1,608	5	458	7	336	42	961	99	2,364

4.2. Assessment of Retrieved Forest GSV with Respect to Forest Inventory Data

Comparisons of the 1-km ASAR and the 25-m PALSAR GSV estimates with forest inventory showed positive correlations for all test sites, but different congruency levels occurred among the test sites (Table 4). The congruency was weak in Bolshemurtinsk/Kasachinsk and Padunsk with *R* values between 0.3 and 0.45. Moderate correlations were achieved for the Abansk/Dolgomostovsk test site (0.6 and 0.55, respectively). The RMSE between ASAR-based GSV and FI GSV was between 47.7 and 64.9 m³/ha. The RMSE between the PALSAR-based GSV and the FI GSV was between 58.9 and 71.3 m³/ha. For a better comparability between test sites the relative RMSE was included related to the average stocking (167.1 m³/ha) in the FI data. At test site level the ASAR-based map achieves a deviation from FI estimates of 28.39%–38.63% (total mean for all test sites = 34.01%). Slightly higher RMSE show the GSV maps derived from the PALSAR mosaics (35.06%–42.44%, total mean for all test sites = 39.44%).

When stratifying the FI-SAR comparisons according to dominant species, the strongest congruency for both SAR products was achieved for the classes Spruce (1 km GSV: 34.76%, 25 m GSV: 33.96%) and Birch (1 km GSV: 34.96%, 25 m GSV: 35.18%) followed by Larch and Aspen (Figure 4). Species with higher maximum average stocking rates like Pine (1 km GSV: 36.51%, 25 m GSV: 42.86%) and Siberian Pine (1 km GSV: 39.23%, 25 m GSV: 57.96%) indicate better map congruities for the ASAR-based map. Comparisons of the Siberian Pine stands show high incongruities in the Padunsk region. The Siberian Pine error distributions of the other two test sites are comparable with those of the Pine stands. Except for the Padunsk test site the best FI-SAR GSV congruencies were measured in the higher biomass stands of the ASAR-based GSV maps. However, the high stocking stands indicate higher incongruities between the ASAR and the PALSAR-based maps. Generally, Kazachinsk (test

site 1) and Abansk/Dolgomostowsk (test site 2) have similar results in terms of species-wise GSV deviations. Padunsk (test site 3) shows higher errors, particularly for Fir and Siberian Pine. Here, the difference between the ASAR-based and the PALSAR-based GSV products has the highest RMSE at 1 km scale. The FI statistics (Table 3) report most extensive disturbances for the Padunsk test site (5416 ha clear cuts and 1608 ha burned area), causing higher small-scale fragmentation of forest. This may introduce errors at 1 km scale GSV estimates.

Table 4. Comparison of ENVISAT ASAR (1 km) and ALOS PALSAR (25 m, resampled to 1 km) growing stock volume maps with forest inventory data for Bolshemurtinsk/Kasachinsk (1), Abansk/Dolgomostowsk (2), and Padunsk (3). Correlation coefficients, root mean square errors (RMSE), and relative RMSE are shown for each test site (mean values per test site and total mean); RMSE and relative RMSE are shown for the dominant species (mean values per test site and total mean).

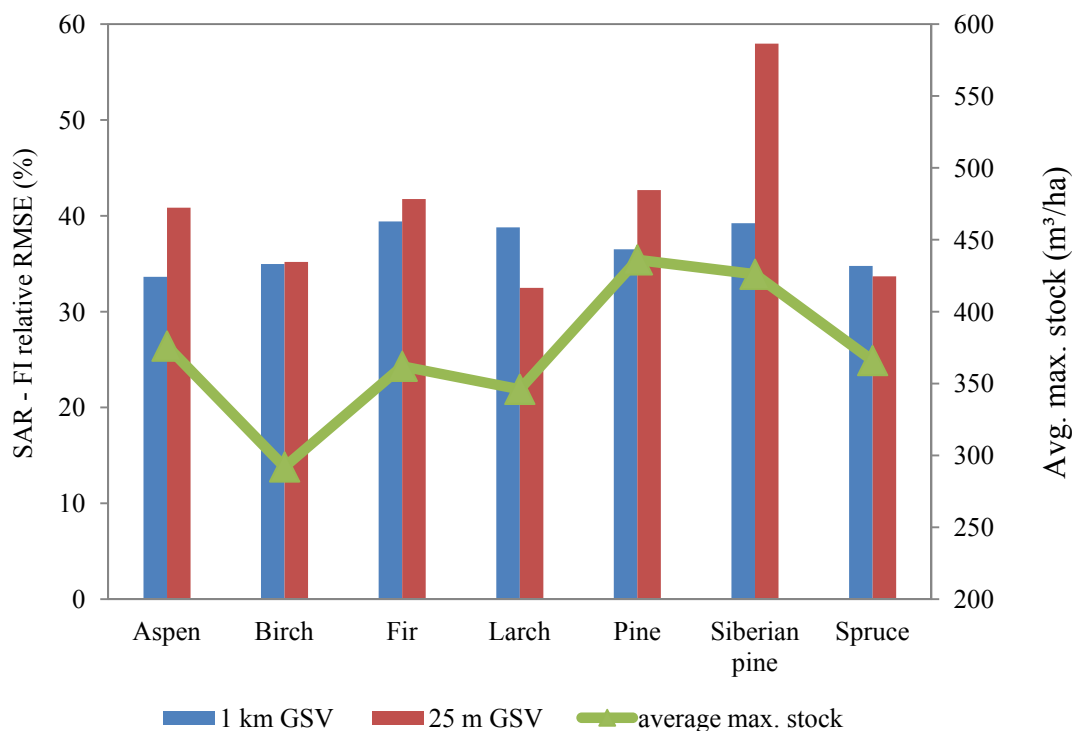
Site	1		2		3		Total Mean	
Overall for Test Sites	1 km	25 m	1 km	25 m	1 km	25 m	1 km	25 m
<i>R</i>	0.34	0.39	0.60	0.55	0.30	0.54	0.41	0.49
RMSE (%)	35.00	40.71	28.39	35.06	38.63	42.44	34.01	39.40
RMSE (m ³ /ha)	58.80	68.40	47.70	58.90	64.90	71.30	57.13	66.20
RMSE (m ³ /ha)	1 km	25 m	1 km	25 m	1 km	25 m	1 km	25 m
Relative RMSE (%) *	1 km	25 m	1 km	25 m	1 km	25 m	1 km	25 m
Aspen	62.50	70.70	46.90	66.00	60.10	69.20	56.50	68.63
	37.20	42.08	27.92	39.29	35.77	41.19	33.63	40.85
Birch	59.10	60.30	48.00	55.00	69.10	62.00	58.73	59.10
	35.18	35.89	28.57	32.74	41.13	36.90	34.96	35.18
Fir	57.70	78.00	46.00	65.90	94.90	66.50	66.20	70.13
	34.35	46.43	27.38	39.23	56.49	39.58	39.40	41.75
Larch	57.40	53.10	75.10	55.00	63.00	55.60	65.17	54.57
	34.17	31.61	44.70	32.74	37.50	33.10	38.79	32.48
Pine	76.10	72.30	47.70	63.70	60.20	79.10	61.33	71.70
	45.30	43.04	28.39	37.92	35.83	47.08	36.51	42.68
Siberian pine	52.10	92.50	53.10	99.80	92.50	99.80	65.90	97.37
	31.01	55.06	31.61	59.40	55.06	59.40	39.23	57.96
Spruce	44.20	62.30	42.30	52.40	88.70	55.10	58.40	56.60
	26.31	37.08	25.18	31.19	52.80	32.80	34.76	33.69

* Relative RMSE in % related to the average stocking on FI stand level of 167.1 (m³/ha).

To get an understanding of the spatial distribution of the discrepancies between the FI dataset and the two SAR-based datasets of GSV, difference maps of the SAR-based GSV maps and the forest inventory were generated. SAR—FI difference maps are given for the three test sites in Figure 5. The images depict similar patterns of over- and underestimation for the resolution levels of 25 m and 1 km, *i.e.*, a lower representation of GSV derived from FI in the surrounding of Abansk (Figure 5b) or lower SAR GSV retrievals in the Dolgomostowsk district (Figure 5a), detected for both pixel spacing resolutions. Except of the comparisons in Figure 5a (Bolshemurtinsk) the SAR GSV retrievals indicate consistent maps of the GSV distribution. The observed high deviations between the SAR GSV

mapping results in the western Bolshemurtinsk region can be explained with effects of SAR image mosaicking where in this region comparable lower backscatter values occur.

Figure 4. Relative RMSE of SAR—forest inventory comparisons of dominant forest species (mean values of all test sites); the 1 km GSV map better matches with FI in the high biomass levels and vice versa.



4.3. Cross-Comparison of SAR-Based GSV Datasets

Both SAR estimates show an overestimation in the low GSV areas and underestimation in the high GSV areas (Figure 6). To get a better understanding of the two SAR-based estimates and increase our understanding of the discrepancies with respect to the FI data, the SAR-based estimates of GSV were cross-compared (Figure 7), also with regard to forest land cover classes. The total RMSE for the test sites was 51.62 m³/ha (Bolshemurtinsk/Kazachinsk), 46.07 m³/ha (Abansk/Dolgomostovsk), and 45.68 m³/ha (Padunsk). Relative RMSE was 30.91%, 27.59% and 27.46%. The SAR-based GSV comparisons generally show a better correlation compared to the FI-SAR comparisons, where increased RMSE deviations between the test sites could be reported. The lower saturation stadium for the PALSAR-based GSV maps compared to the ASAR-derived map is visible for all test sites and land cover classes. This is supported by deviations from the 1:1 line of the high volume biomass classes in favor to the ASAR-based map.

Figure 5. Difference of the 1 km GSV (**left**) and 25 m GSV (**right**) maps with respect to the inventory map for the test sites of Kazachinsk and Bolshemurtinsk (**a**), Abansk and Dolgomostovsk (**b**), and Padunsk (**c**).

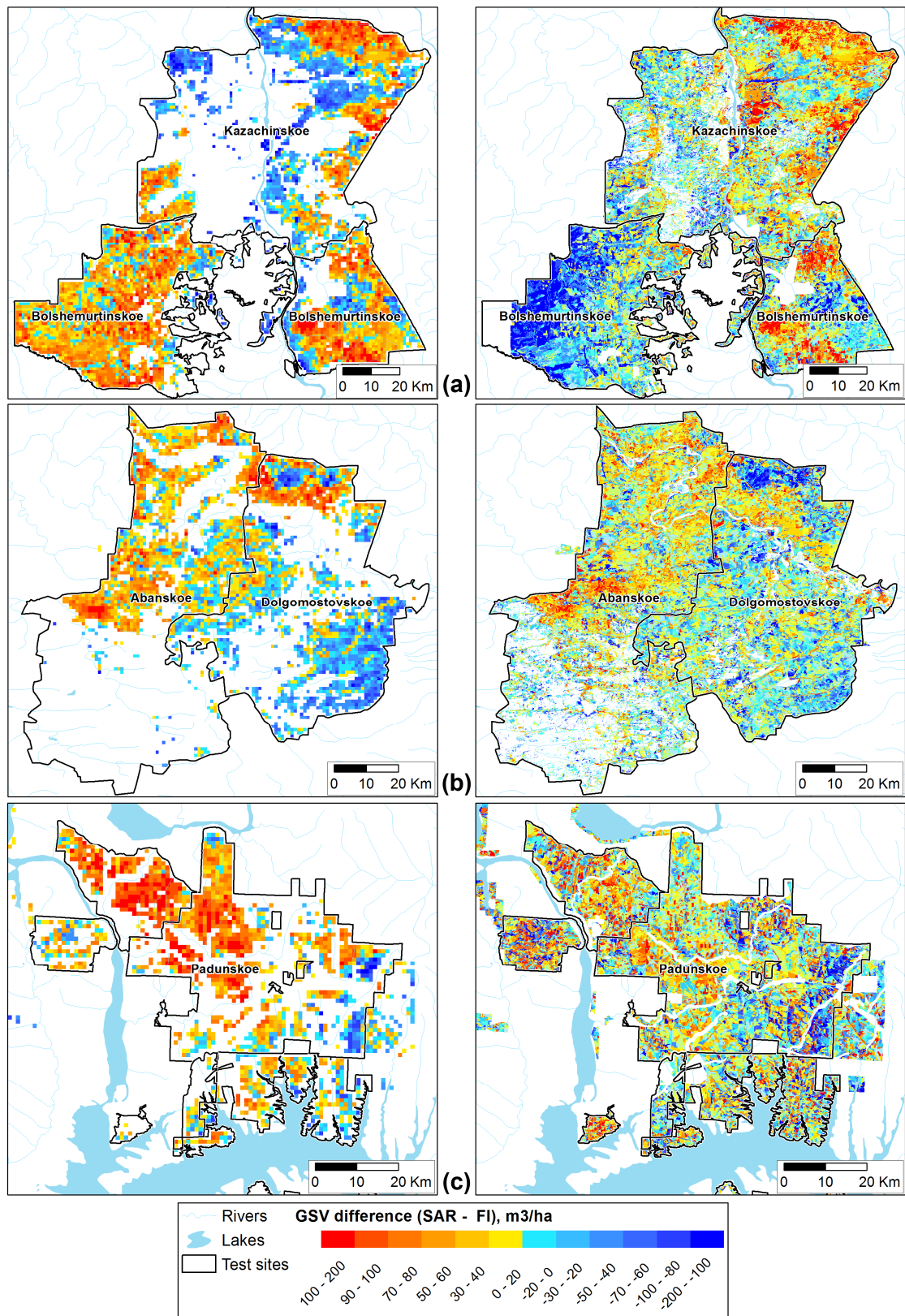
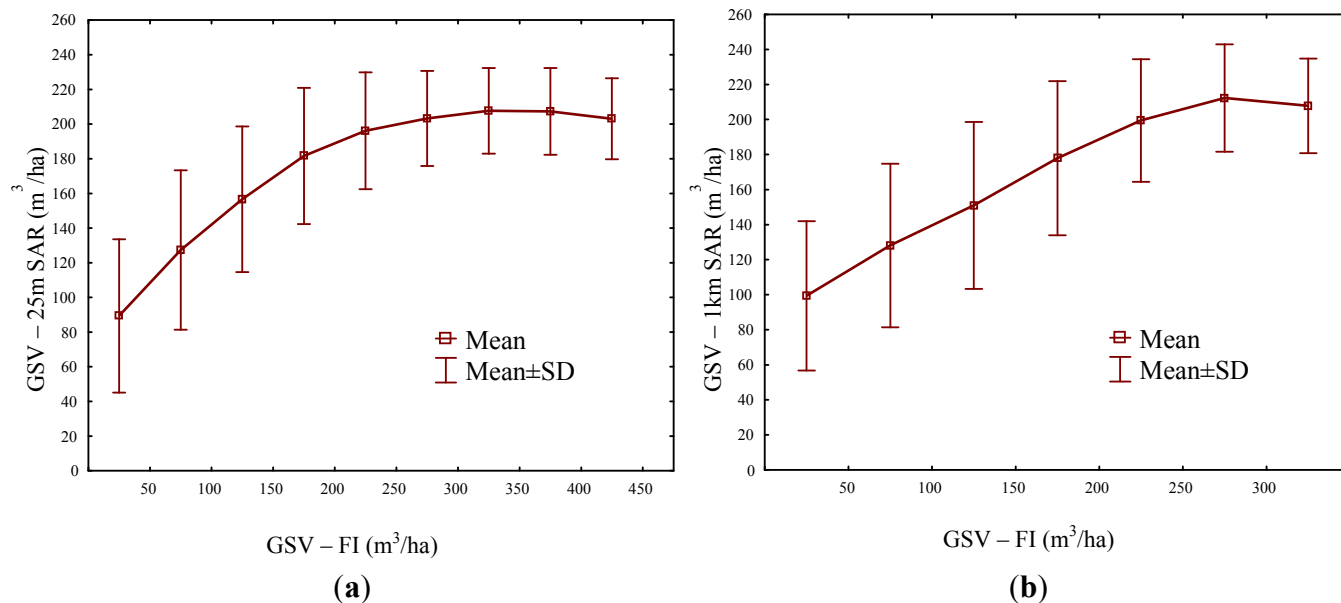


Figure 6. Correlation between growing stock volume and forest inventory and 25 m SAR GSV (a) and 1 km SAR GSV (b) for all test sites.



Class-wise land cover comparisons are shown in Figure 7 to assess whether RMSE discrepancies between ASAR and PALSAR could be explained in terms of forest types. The strongest congruency between the SAR-based datasets of GSV was obtained for *Evergreen-Dark Needleleaf Forest* (RMSE = 31.29 m³/ha and 40.45 m³/ha at Bolshemurtinsk/Kazachinsk and Abansk/Dolgomostowsk). Even higher RMSE values were achieved in the Padunsk test site (45.47 m³/ha). Land cover types consisting of mixed (deciduous and evergreen) forest types or more open forest cover types show higher RMSE and increased variations between test sites than mature forests. Particularly in the Bolshemurtinsk test site, increased scattering in the open forest types can be observed.

Cross-comparisons of the GSV retrievals from FI, ASAR, and PALSAR show distinct differences of the GSV congruency between the three test sites. In order to depict the most consistent dataset between the test sites the RMSE of the three combinations (FI vs. ASAR, FI vs. PALSAR, ASAR vs. PALSAR) are presented in Figure 8. The ASAR and PALSAR GSV estimates comparisons indicate the best map matching among the test sites. As discussed, Bolshemurtinsk/Kazachinsk achieved significantly higher errors than the remaining test regions. Variance in the error distribution is visible within the FI-SAR comparisons for both, between test sites and SAR products. As discussed, the ASAR-based map represents closer results to the FI reference than PALAR. However, the FI-SAR comparisons show substantial inconsistencies between the test sites. The highest errors are observed for Padunsk (which is in contrast to the ASAR-PALSAR comparisons), followed by Bolshemurtinsk/Kazachinsk and Abansk/Dolgomostowsk. The latter test site comes out as most consistent for all comparisons.

Figure 7. Scatterplots showing GSV map congruencies between 25 m and 1 km mapping scales per land cover class for three test sites in central Siberia.

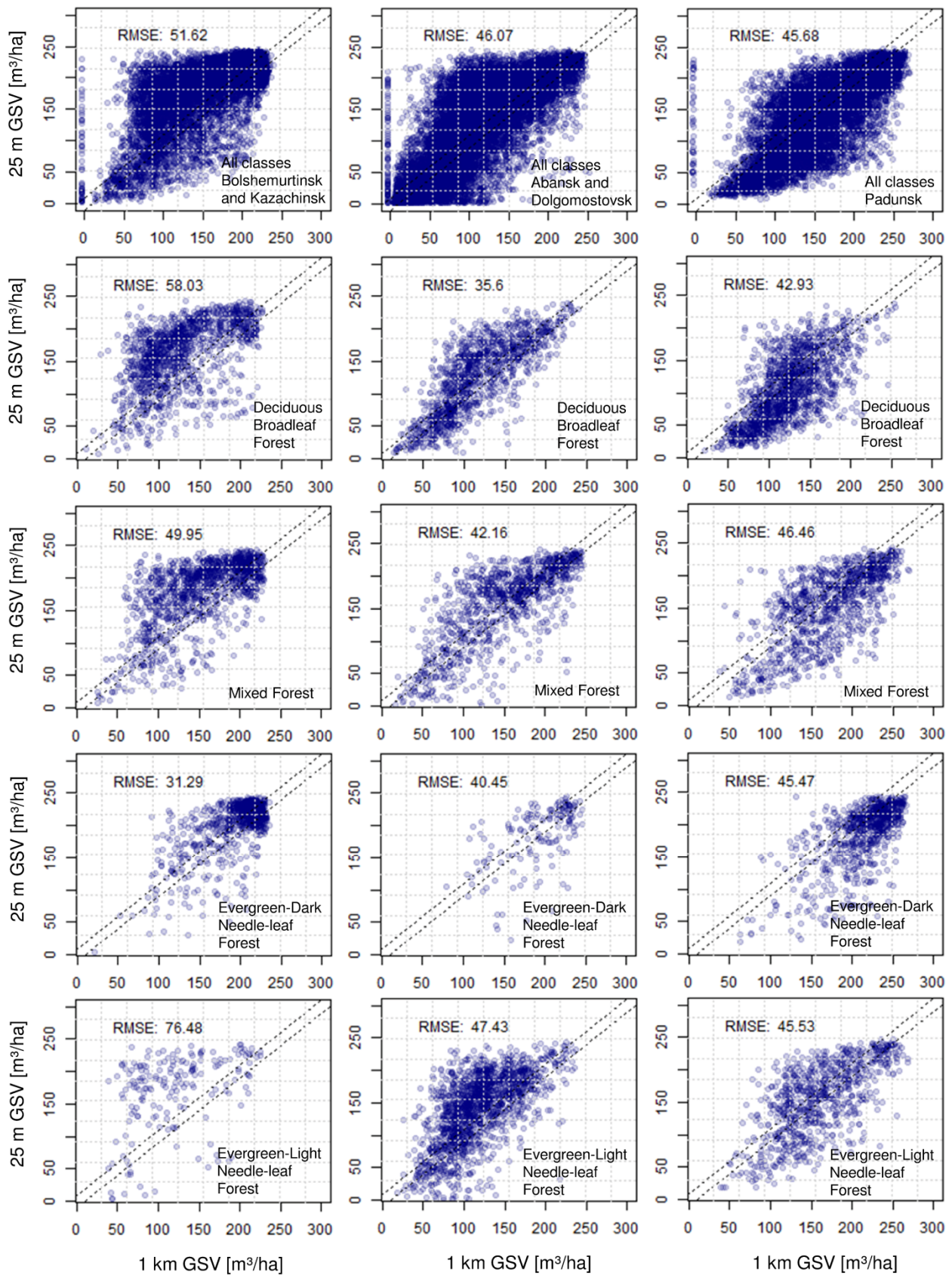
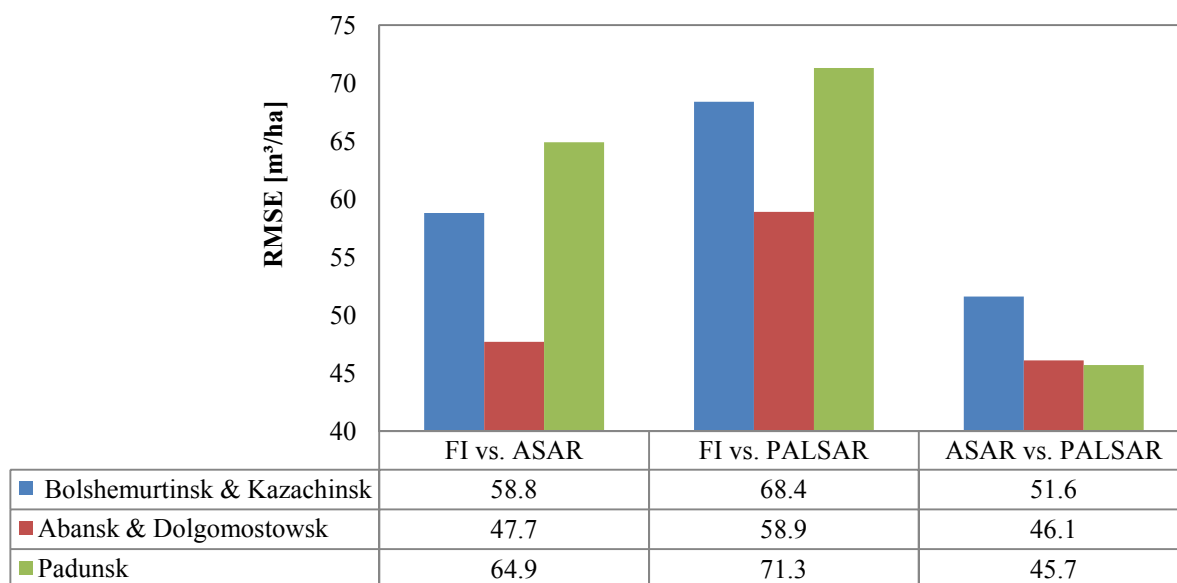


Figure 8. Cross-comparisons of the GSV retrievals from forest inventory, ASAR-based mapping and PALSAR- based mapping.



4.4. Land Cover Distribution Effects on Growing Stock Volume Estimation and Map Congruity

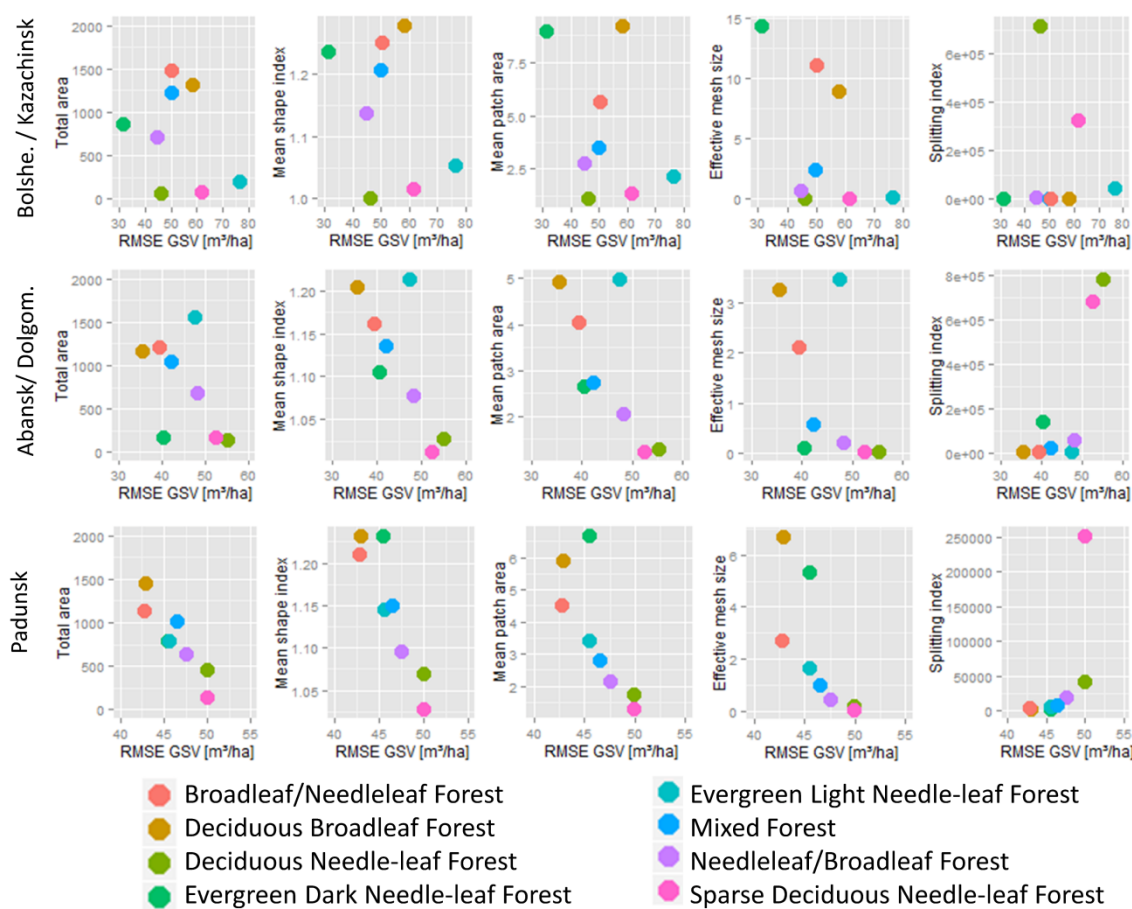
The multi-scale cross-comparisons clearly indicate that the spatial distribution of the forest cover types or landscape distribution is influencing the GSV map matching. Fragmentation indices derived from the MODIS land cover map help to assess these effects on a per class basis. Class-specific GSV RMSE estimates were compared to a selected set of landscape metrics (mean shape index, mean patch area, effective mesh size, and splitting index). Shape index measures the complexity of patch shape compared to a standard shape. Mean shape index measures the average patch shape for a particular class or for all patches in the landscape. This implies a strong impact of the areal extent of the land cover class in the landscape on the deviations of the GSV estimates in the two GSV products. Mean patch size indicates the mean size of all patches for a specific landscape class [44]. Mesh size and splitting index characterize the fragmentation of an area independent of their size and can be used for comparisons of different landscapes. These indices are useful for forest fragmentation analyses in forest landscapes and monitoring changes of the land cover types [45].

The class-wise GSV RMSE estimates show a clear linear trend for the Padunsk test site (Figure 9). Obviously, this is the test site with the best match between the ASAR—PALSAR comparisons. Abansk/Dolgomostowsk shows a similar distribution except for two outlier classes (*Evergreen Dark Needle-leaf Forest* and *Evergreen Light Needle-leaf Forest*). No correlation is visible in the Bolshemurtinsk/Dolgomostowsk test site. The linearity of the fragmentation indices is linked with the distribution of the total area and the RMSE of the ASAR—PALSAR comparisons. The best correlation of total area and RMSE GSV shows Padunsk, which achieved the best ASAR—PALSAR coherence.

The distribution of all fragmentation indices is connected to the land cover area distribution of the multi-scale GSV RMSE. Padunsk shows a normally distributed scattering of GSV with similar deviations from the 1:1 line, whereas the other test sites show an overrepresentation of GSV with regard to the ASAR- based map for all forest classes. By analyzing the fragmentation indices it is

obvious that the forest types with high RMSE measures also show increased fragmentation rates. This is particularly indicated by the splitting index indicating increased fragmentation rates for *Deciduous Needle-leaf Forest* and *Sparse Deciduous Needle-leaf Forest*. *Deciduous Broadleaf Forests*, *Broadleaf/Needleleaf Forests* and *Evergreen Dark Needle-leaf Forests* depict a better connectivity due to a more homogeneous distribution of the forest patches (as indicated by increased values of all fragmentation indices). The Congruency of the GSV estimates between different forest types is determined by the area proportion of the class, the patch area, and the connectivity of the forest class in the landscape. This was indicated by the linear relationship between shape index and GSV congruency.

Figure 9. Scatterplots of landscape metrics derived from the MODIS land cover map and class-specific GSV RMSE between ASAR and PALSAR GSV maps.



5. Discussion

Until now, little knowledge has been acquired to assess the suitability of the different sources of growing stock volume observations for operational forest monitoring and assessment purposes by comparing independently derived SAR-based GSV maps with forest inventory at regional scales. The research question has to be captured, how comparable SAR derived GSV datasets at different scales are and to what extent different SAR-based GSV retrievals fit to forest inventory from different regions. Results of this study show that an interplay of (a) sensor and GSV retrieval method; (b) forest cover type and distribution; and (c) forest inventory in the different forest management areas are affecting the incongruences of the FI-SAR GSV distribution.

5.1. Determinants of Sensor Type and GSV Retrieval Methods

The ASAR- based map shows for all sites with RMSE of 34.01% slightly lower deviations than the ALOS PALSAR product (39.4%). The product cross-comparisons varied between 45.7 and 51.6 m³/ha for all sites. Map matches with a RMSE difference of 5.9 m³/ha between the test sites were achieved despite of the fact that (a) different SAR systems were used (L-band vs. C-band), (b) different temporal resolutions were compared (hyper-temporal ENVISAT-ASAR data vs. annual ALOS-PALSAR mosaic data), and (c) different GSV retrieval methods were applied on the data. The GSV maps correlate well in the average GSV levels. Due to the higher SAR backscatter saturation level the hyper-temporal retrieval approach applied on the ASAR time series shows a general better performance in the mature forests. The advantage of the BIOMASAR algorithm is that it is independent of GSV training data as it is calibrated using literature values and MODIS vegetation continuous field data and estimating the central GSV tendency by using temporal statistics from the multi-temporal backscatter data [14]. The cross-comparisons proved a general consistency of large-scale ALOS PALSAR-based GSV estimation. Some artifacts of striping due to weather or calibration effects were detected in parts of the PALSAR HH and HV mosaics, leading to local inconsistencies in the GSV estimates as also found by [46] and [47]. From a monitoring perspective, acceptable results were achieved with the ALOS-PALSAR and ENVISAT-ASAR derived GSV maps. The random forest regressions used for the ALOS-PALSAR backscatter modeling rely on the GSV training data, which is a disadvantage for product updates and for an operationalization of the mapping framework. This highlights a general disadvantage of supervised modeling approaches. Model calibration of multi-temporal backscatter data is a critical issue since forest inventory is conducted periodically. For instance in remote and inaccessible areas of Central Siberia a frequent FI update is challenging and outdated FI data can be the major source of error for the remotely sensed GSV estimation. Research activities according to [11] have to be intensified to support GSV retrieval algorithms independent of *in situ* data.

5.2. Determinants of Forest Cover Type and Distribution

For most of the sites a good correlation was achieved between the multi-scale products for the *Evergreen-dark Needle-leaf Forests*. Stronger variances occur in the mixed and *Evergreen-light needle-leaf Forest* types. This observation correlates with the GSV map comparisons to forest inventory units. Soil moisture affects the correlation between backscatter and biomass in areas with low biomass levels (e.g., forest regrowth), as found in [48]. This might be a reason for the increased RMSE for the *Sparse Light Needle-leaf Forest* classes. Fragmentation analyses can help to detect local and forest type specific deviations of the spatial GSV distribution of different GSV map products since the fragmentation indices used in this study perform well if the GSV follows a normally distributed shape. Over- or underrepresentation of one product (or in a specific area) results in non-linear distributions of the fragmentation indices compared to the RMSE of two GSV maps. The integration of an auxiliary land cover map helps to detect the forest classes affected by GSV mismatches. Testing independent GSV maps on the linear distribution of RMSE on class level can thus be used to test the general consistency of forest resource information. However, further research has to be conducted to analyze the effect of forest fragmentation and GSV distribution on a landscape level.

5.3. Fostering SAR-Based GSV Assessments for Central Siberian Forest Inventory Support

Compared to the SAR-based RMSE variations between the test sites (5.9 m³/ha), the variations of the RMSE of the FI-SAR comparisons appeared to be higher (Bolshemurtinsk/Kazachinsk: 9.6 m³/ha, Abansk/Dolgomostovsk: 11.2 m³/ha, Padunsk: 6.4 m³/ha). Although an intensive FI update was conducted and up to 5% of 120,636 forest inventory units were excluded from the comparisons, the increased FI-SAR RMSE variations indicate a principal inconsistency of the *in situ* data used in this study. However, SAR-based GSV assessments can be an important information source to detect spatial inconsistencies of FI data. Examples are given with the FI-SAR difference maps in Figure 5. Using such maps in the operational forest management can help to detect forest cover change areas.

Figure 10. Mapping region of the 25 m ALOS PALSAR growing stock volume map (upper image); spatial resolution effects are shown for three examples for 25 m spatial resolution (A–C) and 1 km spatial resolution (D–F).

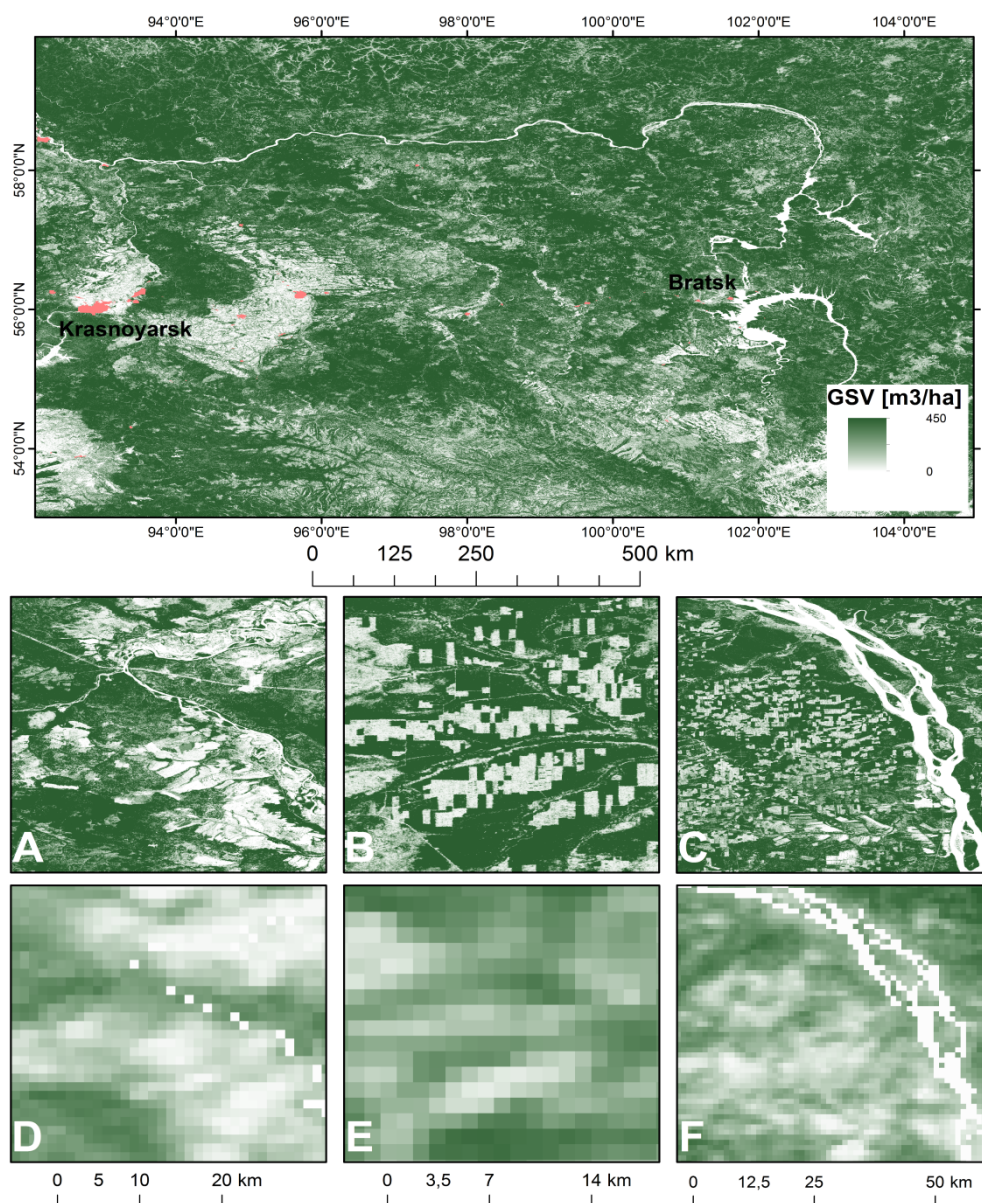


Figure 10 visualizes the full extent of the 25 m resolution GSV map. Compared to the ASAR-based map, both products indicate the suitability for large scale forest monitoring. In fact, the 1 km scale is not appropriate for tracking forest change at the local scale. As Figure 10 shows, land use patterns such as agricultural lands (a and d) and large-scale deforestation areas (b–f) are represented as mixed pixel information. For an operational spatially explicit forest change tracking we recommend a minimum mapping unit of 50 m and smaller. The K&C 25 m PALSAR mosaics have the potential for further global forest monitoring purposes. JAXA recently released a global 50 m backscatter mosaic [49]. This and other operationally processed and globally provided data sources will be key for a spatio-temporally consistent forest change tracking in Boreal ecosystems.

6. Conclusions

Two independently developed large-area GSV maps derived from ENVISAT-ASAR C-band and ALOS PALSAR L-band backscatter data were compared to forest inventory and against each other. Auxiliary land cover data were used and integrated in fragmentation analyses in order to assess class-specific patterns in the GSV distribution in three test sites in Central Siberia covering an area of 1,968,748 ha.

Differences in the GSV distributions of both SAR-based GSV estimates occur (a) between the test sites and (b) between different forest types. Moreover, a general inconsistency in the forest inventory dataset was detected. The forest inventory database turns out to be more inconsistent than the SAR-based GSV maps within the test regions. Following standardized methods and frequent forest inventory updates with comparable error rates is challenging. Reasons for that are for instance the remote and often inaccessible forests in Siberia. However, until now the national forest inventory data are the most important reference information for biomass and growing stock volume mapping and carbon modeling. This study identifies substantial needs for standardized validation methods and guidelines for SAR-based GSV estimates, but also a frequent update of forest inventory on the *in situ* level. This is even more important since forest cover change can be expected to increase in the future (e.g., intensification of logging activities, forest fires, insect outbreaks and permafrost melting).

Implementing integrative concepts of forest resource assessment as shown in Figure 1 could also mean that large scale remotely sensed GSV maps should be used to detect quality gaps in the existing forest inventory databases. Keeping in mind that the update of forest inventory in Siberia is time and cost intensive and a systematic wall-to-wall survey is challenging, the use of SAR-based GSV maps will enhance the future consistency of forest inventory databases. Globally available Radar backscatter mosaic data will be of local relevance in this process. Better spatial and temporal resolution will allow for forest change tracking at local scales with a high spatial and thematic detail. Increasing problems of illegal logging as reported by [50] and [51] can be better quantified and reported in the inventory and located by integrating more frequently updated biomass geo-information.

Upcoming global monitoring programs [20,52] aim at the global quantification of forest biomass distribution to improve resource assessment and carbon accounting, and to foster consistent regional to global vegetation characterization. The methodological toolsets for SAR-based GSV tracking as well as the globally consistent data availability is entering a technical readiness level towards an operational tracking of forest carbon, forest cover change, and growing stock volume. The scientific forest remote

sensing community is entering a new era in earth observation based forests monitoring, where consistent GSV mapping is made possible by spatially consistent and spatio-temporally dense data availability. This situation should be regarded in the national forest inventory strategies.

Acknowledgments

The authors express their thanks to Maurizio Santoro and Tim Robin van Doorn for helpful comments and improvements of the manuscript. This paper was realized in the framework of the FP 7 EU-Russia ZAPÁS project on the assessment and monitoring of forest resources in Central Siberia. ZAPÁS was funded by the European Commission, Space, Cross-cutting Activities, International Cooperation, Grant no. SPA.2010.3.2-01 EU-Russia Cooperation in GMES (SICA). The authors express their thanks to JAXA for providing the 25 m ALOS PALSAR backscatter mosaic data in the framework of the Kyoto and Carbon Science Initiative. Helpful comments and suggestions from the reviewers are highly appreciated.

Author Contributions

Christian Hüttich was responsible for the research design and the editing coordination of the paper. Data preparation and analysis was partitioned as follows: Forest inventory (Mikhail Korets), ALOS-PALSAR GSV maps (Christian Hüttich), ENVISAT-ASAR GSV map (Maurizio Santoro), MODIS land cover map (Sergey Bartalev and Vasily Zharko). Dmitry Schepaschenko and Anatoly Shvidenko gave relevant technical support. Christiane Schmullius provided significant input to the research design. All of the authors contributed in editing and reviewing the manuscript.

Conflicts of Interest

The authors declare no conflict of interest.

References

1. Shvidenko, A.; Schepaschenko, D.; Nilsson, S.; Bouloui, Y. Semi-empirical models for assessing biological productivity of Northern Eurasian forests. *Ecol. Model.* **2007**, *204*, 163–179.
2. Gusti, M.; Jonas, M. Terrestrial full carbon account for Russia: Revised uncertainty estimates and their role in a bottom-up/top-down accounting exercise. *Clim. Chang.* **2010**, *103*, 159–174.
3. Dolman, J.; Shvidenko, A.; Schepaschenko, D.; Ciais, P.; Tchepakova, N.; Chen, T.; van der Molen, M.K.; Beileli Marchesini, L.; Maximov, T.C.; Maksyutov, S.; Schulze, E.-D. An Estimate of the Terrestrial Carbon Budget of Russia Using Inventory-Based, Eddy Covariance and Inversion Methods. *Biogeosciences* **2012**, *9*, 5323–5340.
4. Shvidenko, A.; Schepaschenko, D. Russia faces tough climate change challenges. *Options* **2011**, 18–19.
5. Schepaschenko, D.; See, L.; Fritz, S.; McCallum, I.; Christian, S.; Perger, C.; Baccini, A.; Gallaun, H.; Kindermann, G.; Kraxner, F.; *et al.* Observing forest biomass globally. *Earthzine* **2012**.

6. Shvidenko, A.; Schepaschenko, D.; McCallum, I.; Nilsson, S. Can the uncertainty of full carbon accounting of forest ecosystems be made acceptable to policymakers? *Clim. Chang.* **2010**, *103*, 137–157.
7. Gustafson, E.J.; Shvidenko, A.Z.; Sturtevant, B.R.; Scheller, R.M. Predicting global change effects on forest biomass and composition in south-central Siberia. *Ecol. Appl.* **2010**, *20*, 700–715.
8. Pereira, H.M.; Ferrier, S.; Walters, M.; Geller, G.N.; Jongman, R.H.G.; Scholes, R.J.; Bruford, M.W.; Brummitt, N.; Butchart, S.H.M.; Cardoso, A.C.; *et al.* Essential Biodiversity Variables. *Science* **2013**, *339*, 277–278.
9. Houghton, R.A.; Butman, D.; Bunn, A.G.; Krankina, O.N.; Schlesinger, P.; Stone, T.A. Mapping Russian forest biomass with data from satellites and forest inventories. *Environ. Res. Lett.* **2007**, *2*, 045032.
10. McRoberts, R.E.; Gobakken, T.; Næsset, E. Post-stratified estimation of forest area and growing stock volume using lidar-based stratifications. *Remote Sens. Environ.* **2012**, *125*, 157–166.
11. Powell, S.L.; Cohen, W.B.; Healey, S.P.R.; Kennedy, E.; Moisen, G.G.; Pierce, K.B.; Ohmann, J.L. Quantification of live aboveground forest biomass dynamics with Landsat time-series and field inventory data: A comparison of empirical modeling approaches. *Remote Sens. Environ.* **2010**, *114*, 1053–1068.
12. Tomppo, E.O.; Gagliano, C.; de Natale, F.; Katila, M.; McRoberts, R.E. Predicting categorical forest variables using an improved k-Nearest Neighbour estimator and Landsat imagery. *Remote Sens. Environ.* **2009**, *113*, 500–517.
13. Tomppo, E.; Nilsson, M.; Rosengren, M.; Aalto, P.; Kennedy, P. Simultaneous use of Landsat-TM and IRS-1C WiFS data in estimating large area tree stem volume and aboveground biomass. *Remote Sens. Environ.* **2002**, *82*, 156–171.
14. Santoro, M.; Beer, C.; Cartus, O.; Schmullius, C.; Shvidenko, A.; McCallum, I.; Wegmüller, U.; Wiesmann, A. Retrieval of growing stock volume in boreal forest using hyper-temporal series of Envisat ASAR ScanSAR backscatter measurements. *Remote Sens. Environ.* **2010**, *115*, 490–507.
15. Santoro, M.; Cartus, O.; Fransson, J.; Shvidenko, A.; McCallum, I.; Hall, R.; Beaudoin, A.; Beer, C.; Schmullius, C. Estimates of forest growing stock volume for Sweden, central Siberia, and québec using envisat advanced synthetic aperture radar backscatter data. *Remote Sens.* **2013**, *5*, 4503–4532.
16. Goetz, S.J.; Baccini, A.; Laporte, N.T.; Johns, T.; Walker, W.; Kellndorfer, J.; Houghton, R.; Sun, M. Mapping and monitoring carbon stocks with satellite observations: A comparison of methods. *Carbon Balance Manag.* **2009**, *4*, doi:10.1186/1750-0680-4-2.
17. Cartus, O.; Kellndorfer, J.; Rombach, M.; Walker, W. Mapping canopy height and growing stock volume using airborne lidar, ALOS PALSAR and landsat ETM+. *Remote Sens.* **2012**, *4*, 3320–3345.
18. De Grandi, G.D.; Bouvet, A.; Lucas, R.M.; Shimada, M.; Monaco, S.; Rosenqvist, A. The KC PALSAR mosaic of the African continent: Processing issues and first thematic results. *IEEE Trans. Geosci. Remote Sens.* **2011**, *49*, 3593–3610.

19. Santoro, M.; Schmillius, C.; Pathe, C.; Schwilk, J. Pan-boreal mapping of forest growing stock volume using hyper-temporal Envisat ASAR ScanSAR backscatter data. In Proceedings of the 2012 IEEE International on Geoscience Remote Sensing Symposium (IGARSS), Munich, Germany, 22–27 July 2012; pp. 7204–7207.
20. Seifert, F.M. GlobBiomass—User Consultation Meeting. 2012. Available online: <http://due.esrin.esa.int/meetings/meetings283.php> (accessed on 25 July 2013).
21. Corona, P. Integration of forest mapping and inventory to support forest management. *iForest—Biogeosci. For.* **2010**, *3*, 59–64.
22. Wulder, M.A.; White, J.C.; Fournier, R.A.J.; Luther, E.; Magnussen, S. Spatially explicit large area biomass estimation: Three approaches using forest inventory and remotely sensed imagery in a GIS. *Sensors* **2008**, *8*, 529–560.
23. Blackard, J.; Finco, M.; Helmer, E.; Holden, G.; Hoppus, M.; Jacobs, D.; Lister, A.; Moisen, G.; Nelson, M.; Riemann, R. Mapping U.S. forest biomass using nationwide forest inventory data and moderate resolution information. *Remote Sens. Environ.* **2008**, *112*, 1658–1677.
24. Ryan, B. Introduction to GEO. In Proceedings of the UNFCCC COP-18, Doha, Qatar, 26 November–7 December 2012.
25. Minayeva, L.Y. Forest inventory regulations of Russia. *Mil. Tiprg.* **1995**, *1*, 274.
26. Santoro, M.; Eriksson, L.; Askne, J.; Schmillius, C. Assessment of stand-wise stem volume retrieval in boreal forest from JERS-1 L-band SAR backscatter. *Int. J. Remote Sens.* **2006**, *27*, 3425–3454.
27. Shimada, M.; Ohtaki, T. Generating large-scale high-quality SAR mosaic datasets: Application to PALSAR data for global monitoring. *IEEE J. Sel. Top. Appl. Earth Obs. Remote Sens.* **2010**, *3*, 637–656.
28. Rosenqvist, A.; Ogawa, T.; Shimada, M.; Igarashi, T. Initiating the ALOS Kyoto & Carbon Initiative. In Proceedings of the IEEE 2001 International Geoscience and Remote Sensing Symposium on IGARSS 2001 Scanning the Present and Resolving the Future, Sydney, NSW, Australia, 9–13 July 2001; Volume 1, pp. 546–548.
29. Bartalev, S.A.; Belward, A.S.; Erchov, D.V.; Isaev, A.S. A new SPOT4-VEGETATION derived land cover map of Northern Eurasia. *Int. J. Remote Sens.* **2003**, *24*, 1977–1982.
30. Zharko, V.O.; Bartalev, S.A.; Egorov, V.A. Evaluation of forest tree species composition based on the analysis of their seasonal reflectance dynamic using satellite data (in Russian). In Proceedings of the Tenth Annual All Russian Open Conference Actual Problems in Remote Sensing of the Earth from Space, Moscow, Russia, 12–16 November 2012; p. 386.
31. FFSR. *Manual on forest inventory and planning in forest fund of Russia. Part 1. Organization of forest inventory and field works*; Federal Forest Service of Russia: Moscow, Russia, 1995; pp. 174.
32. Prasad, M.; Iverson, L.R.; Liaw, A. Newer classification and regression tree techniques: Bagging and random forests for ecological prediction. *Ecosystem* **2006**, *9*, 181–199.
33. Gislason, P.; Benediktsson, J.; Sveinsson, J. Random Forests for land cover classification. *Pattern Recognit. Lett.* **2006**, *27*, 294–300.
34. Cutler, D.R.; Edwards, T.C.; Beard, K.H.; Cutler, A.; Hess, K.T.; Gibson, J.; Lawler, J.J. Random forests for classification in ecology. *Ecology* **2007**, *88*, 2783–2792.

35. Hüttich, C.; Herold, M.; Strohbach, B.J.; Dech, S. Integrating *in situ*-, Landsat-, and MODIS data for mapping in Southern African savannas: Experiences of LCCS-based land-cover mapping in the Kalahari in Namibia. *Environ. Monit. Assess.* **2010**, *176*, 531–547.
36. Simard, M.; Pinto, N.; Fisher, J.B.; Baccini, A. Mapping forest canopy height globally with spaceborne lidar. *J. Geophys. Res.* **2011**, *116*, 1–12.
37. Carreiras, J.; Melo, J.; Vasconcelos, M. Estimating the above-ground biomass in Miombo savanna woodlands (Mozambique, East Africa) using L-band synthetic aperture radar data. *Remote Sens.* **2013**, *5*, 1524–1548.
38. Breiman, L.; Friedman, J.H.; Olshen, R.A.; Stone, C.J. *Classification and Regression Trees*; CRC Press: Boca Raton, FL, USA, 1984; pp. 368.
39. Imhoff, M.L. Radar backscatter and biomass saturation: Ramifications for global biomass inventory. *IEEE Trans. Geosci. Remote Sens.* **1995**, *33*, 511–518.
40. Wagner, W. Large-scale mapping of boreal forest in SIBERIA using ERS tandem coherence and JERS backscatter data. *Remote Sens. Environ.* **2003**, *85*, 125–144.
41. Santoro, M.; Shvidenko, A.; Mccallum, I.; Askne, J.; Schmullius, C. Properties of ERS-1/2 coherence in the Siberian boreal forest and implications for stem volume retrieval. *Remote Sens. Environ.* **2007**, *106*, 154–172.
42. Bartalev, S.A.; Egorov, V.A.; Loupian, E.A.; Khvostikov, S.A. A new locally-adaptive classification method LAGMA for large-scale land cover mapping using remote-sensing data. *Remote Sens. Lett.* **2014**, *5*, 55–64.
43. Bartalev, S.A.; Egorov, V.A.; Ershov, D.V.; Isaev, A.S.; Loupian, E.A.; Plotnikov, D.E.; Uvarov, I.A. The vegetation mapping over Russia using MODIS spectroradiometer satellite data. *Contemp. Earth Remote Sens. Sp.* **2011**, *8*, 285–302.
44. McGarigal, K.; Cushman, S.A.; Neel, M.C.; Ene, E. FRAGSTATS: Spatial pattern analysis program for categorical maps. *Computer Software Program Produced by the Authors at the University of Massachusetts*; University of Massachusetts: Amherst, United States of America, 2002; p. 171.
45. Jaeger, J.A.G. Landscape division, splitting index, and effective mesh size: New measures of landscape fragmentation. *Landsc. Ecol.* **2000**, *15*, 115–130.
46. Rauste, Y. Multi-temporal JERS SAR data in boreal forest biomass mapping. *Remote Sens. Environ.* **2005**, *97*, 263–275.
47. Thiel, C.; Schmullius, C. Investigating the impact of freezing on the ALOS PALSAR InSAR phase over Siberian forests. *Remote Sens. Lett.* **2013**, *4*, 900–909.
48. Kasischke, E.S.; Tanase, M.A.; Bourgeau-Chavez, L.L.; Borr, M. Soil moisture limitations on monitoring boreal forest regrowth using spaceborne L-band SAR data. *Remote Sens. Environ.* **2011**, *115*, 227–232.
49. JAXA. New Global 50 m-Resolution PALSAR Mosaic and Forest/Non-Forest Map (2007–2010). Available online: http://www.eorc.jaxa.jp/ALOS/en/palsar_fnf/fnf_index.htm (accessed on 12 May 2014).
50. Kuemmerle, T.; Chaskovskyy, O.; Knorn, J.; Radeloff, V.C.; Kruhlov, I.; Keeton, W.S.; Hostert, P. Forest cover change and illegal logging in the Ukrainian Carpathians in the transition period from 1988 to 2007. *Remote Sens. Environ.* **2009**, *113*, 1194–1207.

51. Hain, H.; Ahas, R. The structure and estimated extent of illegal forestry in Estonia 1998–2003. *Int. For. Rev.* **2005**, *7*, 90–100.
52. Le Toan, T.; Quegan, S.; Davidson, M.W.J.; Balzter, H.; Paillou, P.; Papathanassiou, K.; Plummer, S.; Rocca, F.; Saatchi, S.; Shugart, H.; *et al.* The BIOMASS mission: Mapping global forest biomass to better understand the terrestrial carbon cycle. *Remote Sens. Environ.* **2011**, *115*, 2850–2860.

© 2014 by the authors; licensee MDPI, Basel, Switzerland. This article is an open access article distributed under the terms and conditions of the Creative Commons Attribution license (<http://creativecommons.org/licenses/by/3.0/>).